



## Site occupation evolution of alloying elements in $\text{Ni}_3\text{V}$ phase during phase transformation in $\text{Ni}_{75}\text{Al}_{4.2}\text{V}_{20.8}$

Ming-yi ZHANG<sup>1,2,3</sup>, Zhi-gang LI<sup>2</sup>, Jin-ling ZHANG<sup>2</sup>, Hui-zhan ZHANG<sup>2</sup>, Zhen CHEN<sup>3</sup>, Jia-zhen ZHANG<sup>2</sup>

1. Institute of Fluid Physics, China Academy of Engineering Physics, Mianyang 621900, China;

2. Beijing Aeronautical Science & Technology Research Institute,

Commercial Aircraft Corporation of China, Ltd., Beijing 100083, China;

3. State Key Laboratory of Solidification Processing, Northwestern Polytechnical University, Xi'an 710072, China

Received 5 November 2013; accepted 4 March 2014

**Abstract:** Based on the microscopic phase-field model, the correlation between site occupation evolution of alloying elements in  $\text{Ni}_3\text{V}$ - $\text{DO}_{22}$  phase and growth of  $\text{Ni}_3\text{Al}$ - $\text{L}_{12}$  phase was studied during the phase transformation of  $\text{Ni}_{75}\text{Al}_{4.2}\text{V}_{20.8}$ . The results demonstrate that the growth of  $\text{L}_{12}$  phase can be divided into two stages: at the early stage, the composition of alloying elements in  $\text{DO}_{22}$  phase almost remains unchanged; at the late stage, the compositions of Ni and Al decrease while V increases in  $\text{DO}_{22}$  phase. Part of alloying elements for  $\text{L}_{12}$  phase growth are supplied from the site occupation evolution of alloying elements on three kinds of sublattices in  $\text{DO}_{22}$  phase. Ni is mainly supplied from V sublattice, and part of Al is supplied from  $\text{Ni}_1$  and V sites at the centre of  $\text{DO}_{22}$  phase. The excessive V from the decreasing  $\text{DO}_{22}$  phase migrates into the centre of  $\text{DO}_{22}$  phase and mainly occupies V and  $\text{Ni}_{\text{II}}$  sites. It is the site occupation evolution of antisite atoms and ternary additions in  $\text{DO}_{22}$  phase that controls the growth rate of  $\text{L}_{12}$  phase at the late stage.

**Key words:**  $\text{Ni}_{75}\text{Al}_{4.2}\text{V}_{20.8}$  alloy; grain growth; phase transformation; microscopic phase-field; antisite defect

### 1 Introduction

Extensive studies on the site occupation behavior (including both the site preference of ternary substitution elements and antisites of the constituent elements) of alloying elements were carried out both experimentally and theoretically, because their effects on physical properties of intermetallic compounds are subjects not only of great practical interests but also of fundamental theoretical interests [1]. Site preference of alloying elements can be affected by changing temperature [2], composition [3], or magnetism [4]. The performances of alloys are strongly influenced by site preference of ternary additions and antisite atoms. CHIBA et al [5] found that when the ternary addition preferentially substitutes Ni on the face centered sites in  $\text{Ni}_3\text{Al}$ , the ductility of  $\text{Ni}_3\text{Al}$  can be improved significantly [5]. Studies also demonstrated that site preference of alloying elements severely affects the solute segregation [6,7].

However, little attention has been paid to the correlation between site occupation evolution of alloying elements and phase transformation. An understanding of the site occupation behavior of alloying elements during phase transformation is extremely useful in order to control the microstructure and to improve the physical properties of alloys.

Phase transformation in  $\text{Ni}_{75}\text{Al}_x\text{V}_{25-x}$  alloys during aging process was studied extensively both experimentally [8] and theoretically [9]. Most of the studies are focused on the kinetics of phase separation [10] and microstructure evolution [11]. The atomic ordering and composition clustering process were studied in details by PODURI et al [12] and HOU et al [13]. LI et al [14] investigated the coarsening behavior of  $\text{L}_{12}$  and  $\text{DO}_{22}$  in  $\text{Ni}_{75}\text{Al}_x\text{V}_{25-x}$  alloys systematically, but few studies were focused on the correlation between the behavior of interfaces and phase transformation of  $\text{Ni}_{75}\text{Al}_x\text{V}_{25-x}$  alloys [15,16]. ZHANG et al [17] studied the correlation between the site occupation evolution of

alloying elements in  $L1_2$  phase and the growth of  $DO_{22}$  phase in  $Ni_{75}Al_{7.5}V_{17.5}$ , the mechanism and kinetics of phase transformation from  $L1_2$  to  $DO_{22}$  are delicately investigated at atomistic scale. However, because of the complexity of  $DO_{22}$  crystal structure, little attention has been paid to the site occupation behavior of alloying elements in  $DO_{22}$  [18] and the difference of two kinds of Ni sublattices in  $DO_{22}$  were not considered delicately. The mechanism of phase transformation from  $DO_{22}$  to  $L1_2$  still needs to be further studied at atomic scale. In this work, the site occupation behavior of alloying elements in  $DO_{22}$  phase during phase transformation from  $DO_{22}$  to  $L1_2$  in  $Ni_{75}Al_{7.5}V_{17.5}$  is studied, and their correlation is discussed.

## 2 Microscopic phase-field model

The microscopic phase-field model describes the evolution of site occupation probability from the non-equilibrium distribution to an equilibrium one. It was firstly proposed by KHACHATURYAN [19] and then developed by CHEN and PODURI [12] for the ternary alloy system. Equations for ternary alloy systems are written as

$$\left\{ \begin{array}{l} \frac{dP_A(r,t)}{dt} = \frac{1}{k_B T} \times \\ \sum_{r'} \left[ L_{AA}(r-r') \frac{\partial F}{\partial P_A(r',t)} + L_{AB}(r-r') \frac{\partial F}{\partial P_B(r',t)} \right] \\ \frac{dP_B(r,t)}{dt} = \frac{1}{k_B T} \times \\ \sum_{r'} \left[ L_{BA}(r-r') \frac{\partial F}{\partial P_A(r',t)} + L_{BB}(r-r') \frac{\partial F}{\partial P_B(r',t)} \right] \end{array} \right. \quad (1)$$

For ternary systems,  $P_C(r, t) = 1 - P_A(r, t) - P_B(r, t)$ , where  $P_\alpha(r, t)$  ( $\alpha = A, B$  or  $C$ ) represent the probabilities of finding an  $\alpha$  atom at a given lattice site  $r$  at given time  $t$ , and  $t$  is the reduced time,  $L_{\alpha\beta}(r-r')$  ( $\alpha$  and  $\beta = A, B$  or

$C$ ) are the kinetic coefficients which are proportional to the probabilities of elementary diffusional jumps from site  $r$  to  $r'$  per unit of time, and  $F$  is the total Helmholtz free energy of the system based on the mean-field approximation, which can be written as a function of single site occupation probability:

$$F = -\frac{1}{2} \sum_r \sum_{r'} [V_{AB}(r-r')P_A(r)P_B(r') + V_{BC}(r-r')P_B(r)P_C(r') + V_{AC}(r-r')P_A(r)P_C(r')] + k_B T \sum_r [P_A(r)\ln(P_A(r)) + P_B(r)\ln(P_B(r)) + P_C(r)\ln(P_C(r))] \quad (2)$$

where the effective pair interaction  $V_{\alpha\beta}$  is deduced from pair interaction  $\omega_{\alpha\beta}$ :  $V_{\alpha\beta} = \omega_{\alpha\alpha} + \omega_{\beta\beta} - 2\omega_{\alpha\beta}$ .

For the convenience of analysis and visualization of the atomic configuration and multiphase morphologies, and considering the proper time consumption, numerical simulation was carried out in a 2D square super-cell consisting of  $128 \times 128$  square lattice sites by the projection of 3D crystal structure of  $Ni_3V-DO_{22}$  along the [010] direction. The schematic diagrams of the  $DO_{22}$  crystal structure and the projection of  $DO_{22}$  structure along [010] direction are shown in Figs. 1(a) and (b), respectively.  $DO_{22}$  consists of three kinds of sublattices, and two of them are Ni sites, as denoted as  $Ni_I$  and  $Ni_{II}$ . Both of them contain eight Ni atoms and four V atoms in the first nearest neighbor shell but Ni and V form distinctive coordination geometries. As shown in Figs. 1(c) and (d), the  $Ni_I$  site has four V atoms to form a square configuration and the  $Ni_{II}$  has four V atoms to form a tetrahedral configuration. The number of  $Ni_{II}$  site is two times as many as the  $Ni_I$  site in a  $Ni_3V$  unit cell.

Equation (1) is solved in the reciprocal space using the modified Euler's method with the time increment equal to 0.0002. The real-space atomic site occupation probability of alloying elements is obtained by the Back-Fourier transformation of the solution of Eq. (1). The effective pair interactions (meV/atom) which have

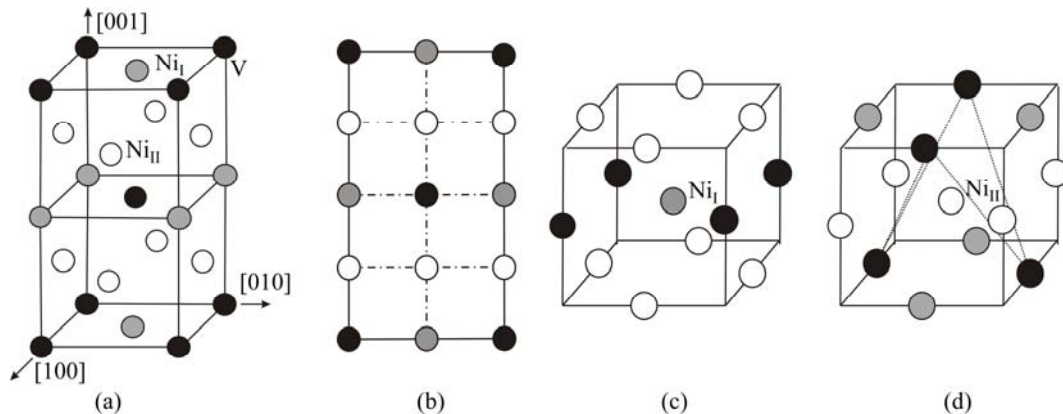


**Fig. 1** Schematic representations of  $Ni_3V$  ( $DO_{22}$ ) crystal structure (a), projection of  $DO_{22}$  structure along [010] direction (b), and first nearest coordination shell and coordination geometry of  $Ni_I$  (c) and  $Ni_{II}$  (d)

been used by PODURI and CHEN [12] and ZAPOLSY et al [20] in the previous works are proved to be fit for the real Ni–Al–V alloy system at high temperatures and are used as our simulation inputs. The applications of microscopic phase-field model on the microstructure evolution of Ni-based alloys had shown excellent agreement both with the experiment results [21] and other simulation results [13].

### 3 Results and discussion

Figure 2 shows the simulated microstructure evolution pictures during the phase transformation of  $\text{Ni}_{75}\text{Al}_{4.2}\text{V}_{20.8}$  alloy aged at 1185 K, where the black sites represent Ni, gray sites represent V and white sites represent Al. It is shown in Fig. 2 that  $\text{L1}_2$  phase grows along the disordered phase at first, and then grows perpendicular to the interface formed between  $\text{L1}_2$  and  $\text{DO}_{22}$  phases.

The volume fraction variation of  $\text{L1}_2$  and  $\text{DO}_{22}$  phases during aging process is shown in Fig. 3, and the volume fraction variation of the disordered phase is also considered. Combined the microstructure evolution pictures with the volume fraction variation figure during the phase transformation, it can be found that the growth of  $\text{L1}_2$  phase can be divided into two stages. At the early stage of phase transformation, the volume of  $\text{L1}_2$  phase increases accompanying with the volume of  $\text{DO}_{22}$  phase and disordered phase decreasing. When the disordered phase disappears,  $\text{L1}_2$  phase grows up at the expense of  $\text{DO}_{22}$  phase only. It is obvious in Fig. 3 that the growth rates of  $\text{L1}_2$  phase at the early stage is higher than that at the late stage.

Further study on the composition evolution of alloying elements in  $\text{DO}_{22}$  phase during phase transformation is shown in Fig. 4(a). Considering the  $\text{DO}_{22}$  phase in the vicinity of interface will transform into  $\text{L1}_2$  phase, only the concentration evolution of alloying elements in the centre part of  $\text{DO}_{22}$  phase is considered. It is demonstrated that at the early stage of  $\text{L1}_2$  phase growth, the concentration of alloying elements in  $\text{DO}_{22}$  phase almost remains unchanged, while at the late stage of phase transformation from  $\text{DO}_{22}$  to  $\text{L1}_2$ , the concentrations of Ni and Al decrease and that of V increases in  $\text{DO}_{22}$  phase. The relationship between the volume fraction of  $\text{L1}_2$  phase and the composition of  $\text{DO}_{22}$  phase (Fig. 4(b)) also illustrates that, the volume fraction of  $\text{L1}_2$  phase increases from about 0 to 0.25 quickly at the early stage, and the composition of the centre part of  $\text{DO}_{22}$  phase almost remains unchanged. At the late stage, the volume fraction of  $\text{L1}_2$  phase grows up slowly from 0.25 to about 0.30, accompanied with the decreasing of Al and Ni concentration, and the increasing of V concentration at the centre part of  $\text{DO}_{22}$  phase. This implies that the growth of  $\text{L1}_2$  phase at the late stage is controlled by the composition evolution of alloying elements in the centre part of  $\text{DO}_{22}$  phase. As mentioned above,  $\text{L1}_2$  phase grows up mainly at the expense of disordered phase at the early stage. Then, it can be concluded that the growth of  $\text{L1}_2$  phase at the early stage is controlled by the diffusion of alloying elements in disordered phases and the growth rate of  $\text{L1}_2$  phase is quick, while the phase transformation at the late stage is controlled by the diffusion of alloying elements in bulk  $\text{DO}_{22}$  phases and the growth rate of  $\text{L1}_2$  phase is relatively slow.

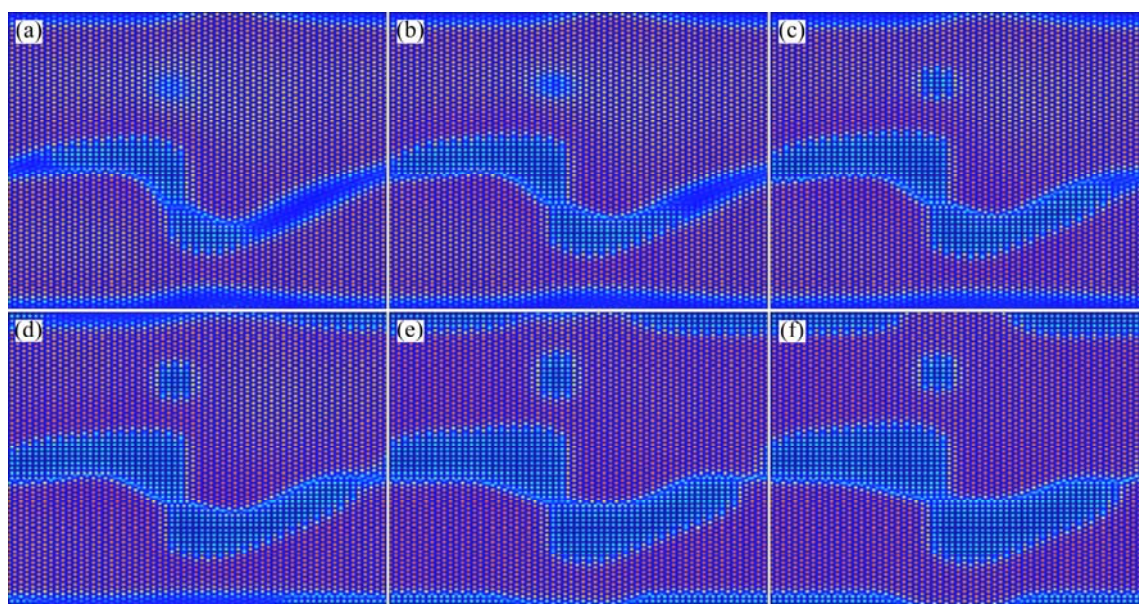


**Fig. 2** Simulated atomistic microstructure evolution figures during phase transformation from disordered (FCC-A1) phase to ordered ( $\text{L1}_2$  and  $\text{DO}_{22}$ ) phase in  $\text{Ni}_{75}\text{Al}_{4.2}\text{V}_{20.8}$  aged at 1185 K: (a)  $t=1.4\times 10^4$ ; (b)  $t=1.6\times 10^5$ ; (c)  $t=1.8\times 10^5$ ; (d)  $t=2.0\times 10^5$ ; (e)  $t=3.0\times 10^5$ ; (f)  $t=4.0\times 10^5$

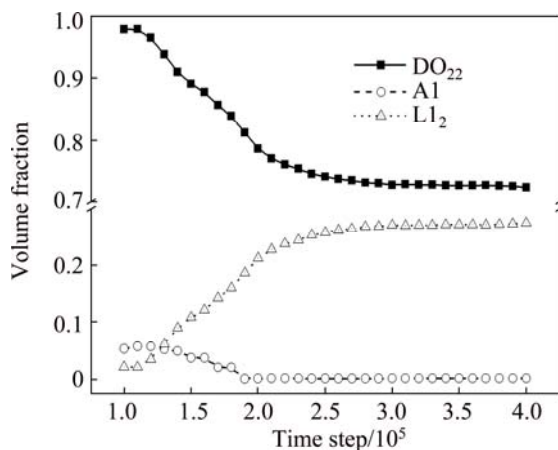


**Fig. 3** Volume fraction variation of  $L_{12}$  and  $DO_{22}$  phase during phase transformation from  $DO_{22}$  to  $L_{12}$  in  $Ni_{75}Al_{4.2}V_{20.8}$  aged at 1185 K

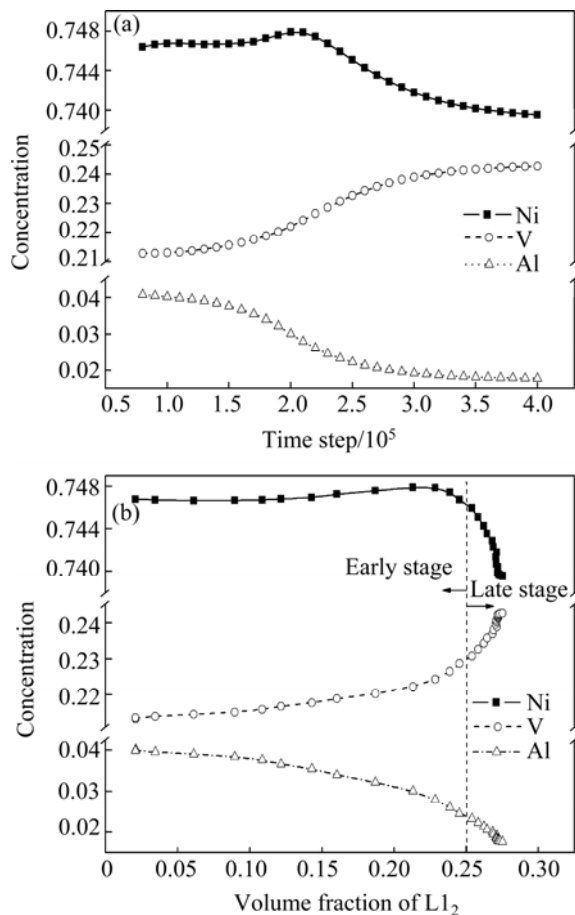


**Fig. 4** Composition evolution of alloying elements in  $DO_{22}$  phase during phase transformation in  $Ni_{75}Al_{4.2}V_{20.8}$  aged at 1185 K: (a) Composition evolution of  $DO_{22}$  phase; (b) Variation of composition of  $DO_{22}$  phase with volume of  $L_{12}$  phase

At the late stage of phase transformation,  $L_{12}$  phase grows up at the expense of  $DO_{22}$  phase, as the growth of  $L_{12}$  phase needs Ni and Al. It was reported that the content of Ni in  $L_{12}$  phase is slightly higher than that in

$DO_{22}$  phase, and the concentration of ternary addition V is about 10% (atomic fraction) in  $L_{12}$  phase [20]. When the volume of  $DO_{22}$  phase is decreasing, alloying elements will be spared from the decreasing  $DO_{22}$  phase. However, the amount of Ni and Al spared from the decreasing  $DO_{22}$  phase are not sufficient for the growth of  $L_{12}$  phase, and the amount of V spared from the decreasing  $DO_{22}$  phase is more than the need of  $L_{12}$  phase growth. Thus, where do the other parts of Al and Ni come from to satisfy the growth of  $L_{12}$ , and where does the enriched V go when the volume of  $DO_{22}$  phase decreases? To answer this question, the composition evolution of alloying elements in  $DO_{22}$  phase is further studied.

It can be seen from Fig. 4 that Ni and Al decrease and V increases with the volume fraction of  $L_{12}$  phase increasing. However, studying on the composition evolution of alloying elements on Ni sites of  $DO_{22}$  phase found that Ni and V increase and Al decreases accompanied with the phase transformation from  $DO_{22}$  to  $L_{12}$ , as shown in Fig. 5. This illustrated that the composition evolution of alloying elements on different sublattices are different, and the composition change of alloying elements on sublattices of  $DO_{22}$  phase are correlated with the phase transformation.

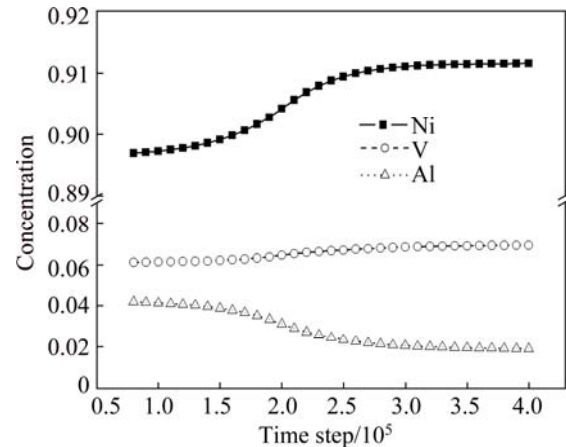


**Fig. 5** Composition evolution of alloying elements on Ni sites of  $DO_{22}$  phase during phase transformation from  $DO_{22}$  to  $L_{12}$  in  $Ni_{75}Al_{4.2}V_{20.8}$  aged at 1185 K

To find out the correlation between the composition evolution of alloying elements in  $DO_{22}$  phase and the growth of  $L_{12}$  phase, the site occupation evolution of alloying elements on three kinds of sublattices of  $DO_{22}$  phase are investigated delicately. Figure 6(a) shows that the site occupation probability of Ni on  $Ni_{I}$  site increases while the site occupation probabilities of Ni on  $Ni_{II}$  and V sites decrease during the phase transformation. The site occupation probability increment of Ni on  $Ni_{I}$  site is larger than the site occupation probability decrement of Ni on  $Ni_{II}$  site, but smaller than the site occupation

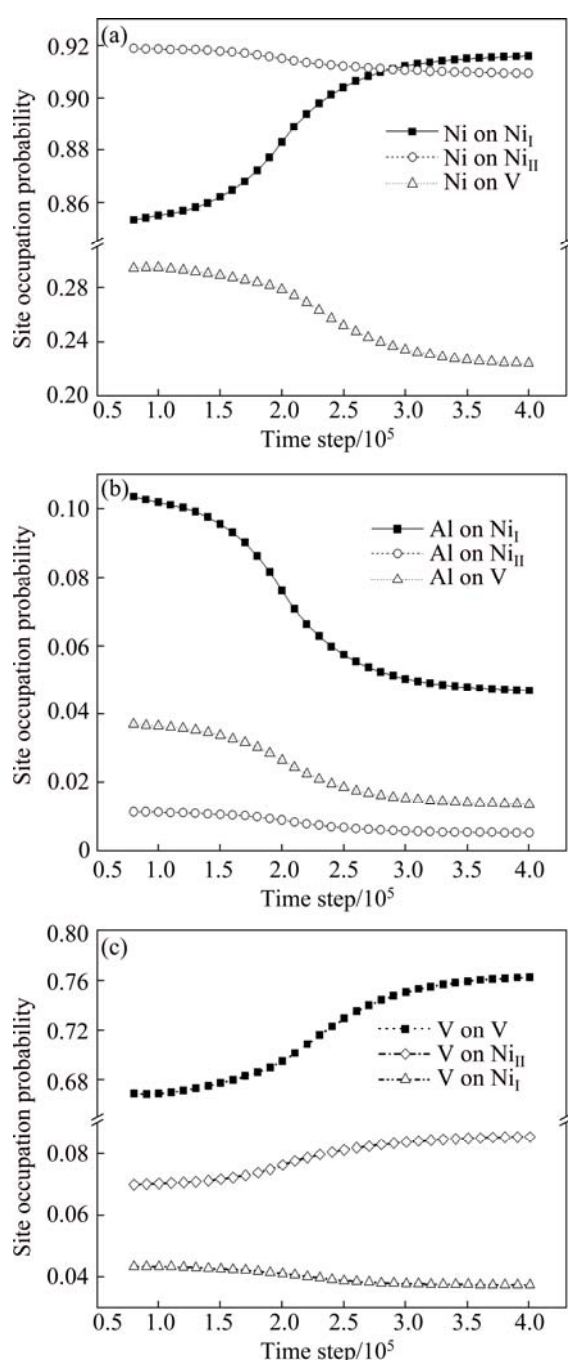


**Fig. 6** Site occupation probability evolution of alloying elements in  $DO_{22}$  phase during phase transformation from  $DO_{22}$  to  $L_{12}$  in  $Ni_{75}Al_{4.2}V_{20.8}$  aged at 1185 K: (a) Ni; (b) Al; (c) V

probability decrement of Ni on V site. Thus, the composition of Ni in  $DO_{22}$  phase decreases while the composition of Ni on Ni sites increases during the growth of  $L_{12}$  phase, as demonstrated in Figs. 4(a) and 5. Figure 6(b) shows that the site occupation probabilities of Al on all three kinds of sublattices of  $DO_{22}$  phase decrease during phase transformation, and the site occupation probabilities decrement of Al on  $Ni_I$  and V sites is obviously larger than that on  $Ni_{II}$  site. For the site occupation probability of V on three kinds of sublattices

of  $DO_{22}$  phase during phase transformation, Fig. 6(c) shows that V increases on V and  $Ni_{II}$  sites, and decreases on  $Ni_I$  site.

It can be concluded from the above results that part of Ni for the growth of  $L_{12}$  phase is supplied from the centre of  $DO_{22}$  phase, and mainly comes from V sublattice. Part of Al for the growth of  $L_{12}$  phase is supplied from  $Ni_I$  and V sites of  $DO_{22}$  phase. The enriched V from the decreasing  $DO_{22}$  phase mainly occupies V and  $Ni_{II}$  sites. In other words, the evolution of antisite atoms and ternary additions in the centre part of  $DO_{22}$  phase contribute to the  $L_{12}$  phase growth at the late stage. And it is the diffusion of antisite atoms and ternary additions from the centre part of  $DO_{22}$  phase to the interfaces of  $DO_{22}$  and  $L_{12}$  phases that controls the growth rate of  $L_{12}$  phase.

## 4 Conclusions

1) The growth of  $Ni_3Al$  phase during the phase transformation of  $Ni_{75}Al_{4.2}V_{20.8}$  alloy can be divided into two stages, based on the volume fraction growth rate of  $L_{12}$  phase, and the relationship between the composition evolution of alloying elements in  $DO_{22}$  phase and the volume fraction of  $L_{12}$  phase.

2) At the early stage, the composition in the centre part of  $DO_{22}$  phase almost remains unchanged,  $L_{12}$  phase grows quickly and it is controlled by the diffusion of alloying elements in disordered phase. At the late stage, the growth of  $L_{12}$  phase is controlled by site occupation evolution of alloying elements in the centre part of  $DO_{22}$  phase, and the growth rate of  $L_{12}$  phase is relatively slow.

3) At the late stage, part of alloying elements for  $L_{12}$  phase growth are supplied from the centre of  $DO_{22}$  phase. Part of Ni is mainly supplied from V sublattice, and part of Al is supplied from  $Ni_I$  and V sites at the centre of  $DO_{22}$  phase. The excessive V from the decreasing  $DO_{22}$  phase migrates into the centre of  $DO_{22}$  phase and mainly occupies V and  $Ni_{II}$  sites.

## References

- [1] PRINS S, ARROYAVE R, LIU Z K. Defect structures and ternary lattice site preference of the B2 phase in the Al–Ni–Ru system [J]. *Acta Materialia*, 2007, 55: 4781–4787.
- [2] JIANG C. Site preference of transition-metal elements in B2 NiAl: A comprehensive study [J]. *Acta Materialia*, 2007, 55: 4799–4806.
- [3] ZHANG J, CHEN Z, LU Y L, ZHANG M Y, WANG Y X. Microscopic phase field study of the antisite defect of  $Ni_3Al$  in binary Ni–Al alloys [J]. *Science China: Physics, Mechanics and Astronomy*, 2010, 53: 2047–2053.
- [4] SLUTIER M H F, KAWAZOE Y. Site preference of ternary additions in  $Ni_3Al$  [J]. *Physical Review B*, 1995, 51: 4062–4073.
- [5] CHIBA A, HANADA S, WATANABE S, ABE T, OBANA T. Relation between ductility and grain boundary character distributions in  $Ni_3Al$  [J]. *Acta Materialia*, 1994, 42: 1733–1738.

- [6] KITASHIMA T, YOKOKAWA T, YEH A C, HARADA H. Analysis of element-content effects on equilibrium segregation at  $\gamma$ - $\gamma'$  interface in Ni-base superalloys using the cluster variation method [J]. *Intermetallics*, 2008, 16: 779–784.
- [7] MOSCA H O, BOZZOLO G, GARCÉS J E. Site preference, size effects and segregation in RuAlB alloys [J]. *Scripta Materialia*, 2008, 58: 1025–1028.
- [8] MARTEAU L, PAREIGE C, BLAVETTE D. Imaging the three orientation variants of the DO<sub>22</sub> phase by 3D atom probe microscopy [J]. *Journal of Microscopy*, 2001, 204: 247–251.
- [9] LI Y S, CHEN Z, LU Y L, WANG Y X. Phase-field simulation of phase separation in Ni<sub>75</sub>Al<sub>x</sub>V<sub>25-x</sub> alloy with elastic stress [J]. *Transactions of Nonferrous Metals Society of China*, 2006, 16(3): 2017–2021.
- [10] TANIMURA M, KOYAMA Y. The role of antiphase boundaries in the kinetic process of the L1<sub>2</sub>→DO<sub>22</sub> structural change of a Ni<sub>3</sub>Al<sub>0.45</sub>V<sub>0.50</sub> alloy [J]. *Acta Materialia*, 2006, 54: 4385–4391.
- [11] PAREIGE C, BLAVETTE D. Simulation of the FCC-FCC+L1<sub>2</sub>+DO<sub>22</sub> kinetic reaction [J]. *Scripta Materialia*, 2001, 44: 243–247.
- [12] PODURI R, CHEN L Q. Computer simulation of atomic ordering and compositional clustering in the pseudobinary Ni<sub>3</sub>Al–Ni<sub>3</sub>V system [J]. *Acta Materialia*, 1998, 46: 1719–1729.
- [13] HOU H, ZHAO Y H, ZHAO Y H. Simulation of the precipitation process of ordered intermetallic compounds in binary and ternary Ni–Al-based alloys by the phase-field model [J]. *Materials Science and Engineering A*, 2009, 499: 204–207.
- [14] LI Y S, CHEN Z, LU Y L, XU G D. Dynamic scaling behaviour of late-stage phase separation in Ni<sub>75</sub>Al<sub>x</sub>V<sub>25-x</sub> alloys [J]. *Chinese Physics B*, 2007, 16: 854–861.
- [15] TANIMURA M, HIRATA A, KOYAMA Y. Kinetic process of the phase separation in the alloy Ni<sub>3</sub>Al<sub>0.52</sub>V<sub>0.48</sub> [J]. *Physical Review B*, 2004, 70: 094111.
- [16] ZHANG M Y, CHEN Z, WANG Y X, MA G, LU Y L, FAN X L. Effect of atomic structure on migration characteristic and solute segregation of ordered domain interfaces formed in Ni<sub>75</sub>Al<sub>x</sub>V<sub>25-x</sub> [J]. *Transactions of Nonferrous Metals Society of China*, 2011, 21: 604–611.
- [17] ZHANG J, CHEN Z, WANG Y X, LU Y L, HUO J L, ZHEN H H, ZHAO Y. Microscopic phase field simulation for the evolution of antisite defect of L1<sub>2</sub> structure and DO<sub>22</sub> structure in Ni<sub>75</sub>Al<sub>5.3</sub>V<sub>19.7</sub> alloy [J]. *Acta Physica Sinica*, 2009, 58: 631–637.
- [18] ZHANG M Y, LIU F, CHEN Z, GUO H J, YUE G Q, YANG K. Site occupation evolution of alloying elements in L1<sub>2</sub> phase during phase transformation in Ni<sub>75</sub>Al<sub>7.5</sub>V<sub>17.5</sub> [J]. *Transactions of Nonferrous Metals Society of China*, 2012, 22: 2439–2443.
- [19] KHACHATURYAN A G. *Theory of structural Transformations in solids* [M]. New York: Wiley, 1983.
- [20] ZAPOLSKY H, PAREIGE C, MARTEAU L, BLAVETTE D, CHEN L Q. Atom probe analyses and numerical calculation of ternary phase diagram in Ni–Al–V system [J]. *Calphad*, 2001, 25: 125–134.

## Ni<sub>75</sub>Al<sub>4.2</sub>V<sub>20.8</sub> 相变过程中 DO<sub>22</sub> 相合金元素 占位几率演化的微观相场模拟

张明义<sup>1,2,3</sup>, 李志刚<sup>2</sup>, 张金玲<sup>2</sup>, 张会占<sup>2</sup>, 陈 铮<sup>3</sup>, 张嘉振<sup>2</sup>

1. 中国工程物理研究院 流体物理研究所, 绵阳 621900;

2. 中国商用飞机有限责任公司 北京民用飞机技术研究中心, 北京 100083;

3. 西北工业大学 凝固技术重点实验室, 西安 710072

**摘 要:** 基于微观相场模型, 研究 Ni<sub>75</sub>Al<sub>4.2</sub>V<sub>20.8</sub> 相变过程中 Ni<sub>3</sub>V-DO<sub>22</sub> 相中合金元素占位几率演化规律与 Ni<sub>3</sub>Al-L1<sub>2</sub> 相长大之间的内在关联。结果表明 L1<sub>2</sub> 相长大过程可以分为两个阶段。在前期, DO<sub>22</sub> 相内合金元素的成分基本保持不变; 在后期, DO<sub>22</sub> 相中 Ni 和 Al 的浓度降低, 而 V 的浓度升高。合金元素在 DO<sub>22</sub> 相中各个格点位置上的浓度发生不同变化; 为 L1<sub>2</sub> 相长大后期提供部分合金元素: 其中, Ni 主要来源于 DO<sub>22</sub> 相中的 V 格点位置; Al 主要来源于 Ni<sub>I</sub> 和 V 格点位置; 由于 DO<sub>22</sub> 相体积减少而富余的 V 向 DO<sub>22</sub> 相内部扩散, 主要占据 V 和 Ni<sub>II</sub> 格点位置。L1<sub>2</sub> 相长大的后期主要受 DO<sub>22</sub> 相内反位缺陷和第三组元的演化所控制。

**关键词:** 镍基合金; 晶粒生长; 相变; 微观相场; 反位缺陷

(Edited by Mu-lan QIN)